

A COMPARAISON OF MEASUREMENTS AND CFD SIMULATIONS FOR POLLUTANT DISPERSION IN URBAN GEOMETRIES

Valeria Garbero¹, Pietro Salizzoni^{1,2}, Lionel Soulhac²,
Patrick Mejean² and Richard Perkins²

¹DIASP, Politecnico di Torino, Corso Einaudi, 24 Torino, Italia

²Laboratoire de Mécanique des Fluides et d'Acoustique, UMR CNRS 5509, Université de
Lyon, Ecole Centrale de Lyon 36, Avenue Guy de Collongue, 69134 Ecully

INTRODUCTION

Squares and street intersections play an important role in pollutant dispersion, as they represent regions of pollutant exchanges between different streets. Recently, different studies pointed out how complicated flow and dispersion patterns are (*Dabbert W. et al.*, 1995) and how much they are sensitive to changes in the intersection geometry (*Robins A. et al.*, 2002; *Wang X. and K. F. McNamara*, 2007).

This paper contains both wind-tunnel and Computational Fluid Dynamics (CFD) investigations of flow and dispersion in two typical urban configurations: the square and the street intersection, consisting of two crossing orthogonal streets. The intersections have been investigated by varying the spacing between the buildings and the results have been compared to those obtained in the case of the square, in order to study the effect of the geometrical layout on the flow dynamics and on the pollutant dispersion. Experimental and numerical data are examined and CFD is evaluated as tool for simulating flow and dispersion in complex geometries.

In the following section the CFD and wind-tunnel set up are described; in the subsequent sections the simulation results are presented and the comparisons are discussed.

WIND TUNNEL AND CFD SIMULATIONS

The wind-tunnel investigations were conducted in a recirculating wind tunnel at the LMFA, Ecole Centrale de Lyon, whose test section is 14 m long x 3.7 m wide x 2.5 m high. A neutrally stratified boundary layer has been generated by means of Irwin spire arrays and roughness elements disposed on the floor, representing an urban atmospheric boundary layer at a scale factor of 1:400. The mean velocity profile was fitted by the typical logarithmic law in the equation (1):

$$U(z) = \frac{u_*}{k} \ln \left(\frac{z-d}{z_0} \right) \quad (1)$$

where the friction velocity was $u_* = 0.27$ m/s, the roughness height $z_0 = 0.5$ mm and the displacement height $d = 35$ mm – values referred to as the model site. The wind tunnel set up consisted in an array of buildings, in order to reproduce a more realistic scenario and to avoid blockage effects, although the investigation has been focused on a single intersection, as shown in Figure 1a. The building-like obstacles measured $H \times 5H \times 5H$, where H was 50 mm, simulating real buildings of 20 m height and 100 m width. The studied configurations, displayed in Figure 1, consisted in a *square* of side $L = 5H$ and spacing $S_x = S_y = 1$ and in three types of *street intersection*, characterised by different spacing between the buildings: $S_x = S_y = H$ (Conf-1), $S_x = 2H$ $S_y = H$ (Conf-2) and $S_x = H$ $S_y = 2H$ (Conf-3). A passive tracer was released from a point source placed within the array at height $z = H/2$. Flow field investigations were performed by means of the Laser Doppler Anemometry, while concentration values

were measured by the Flame Ionisation Detector; non-dimensional mean concentrations are calculated as $K=CUHL/Q$, where C is the mean concentration of the tracer, U the velocity at the roof level, Q the emission rate, H the height and L the length of the buildings.

The numerical simulations were performed by means of the commercial code FLUENT; a standard $k-\epsilon$ turbulence model was implemented. In order to limit the computing time, the numerical domain consisted in a single intersection¹; at the same time, in order to simulate the whole obstacle array, periodical conditions have been set on the inlet and the outlet and conditions of symmetry were set on the top and on the lateral boundaries. The velocity profile obtained through the numerical simulations was similar to the experimental one, assuring the correct representation of the boundary layer processes.

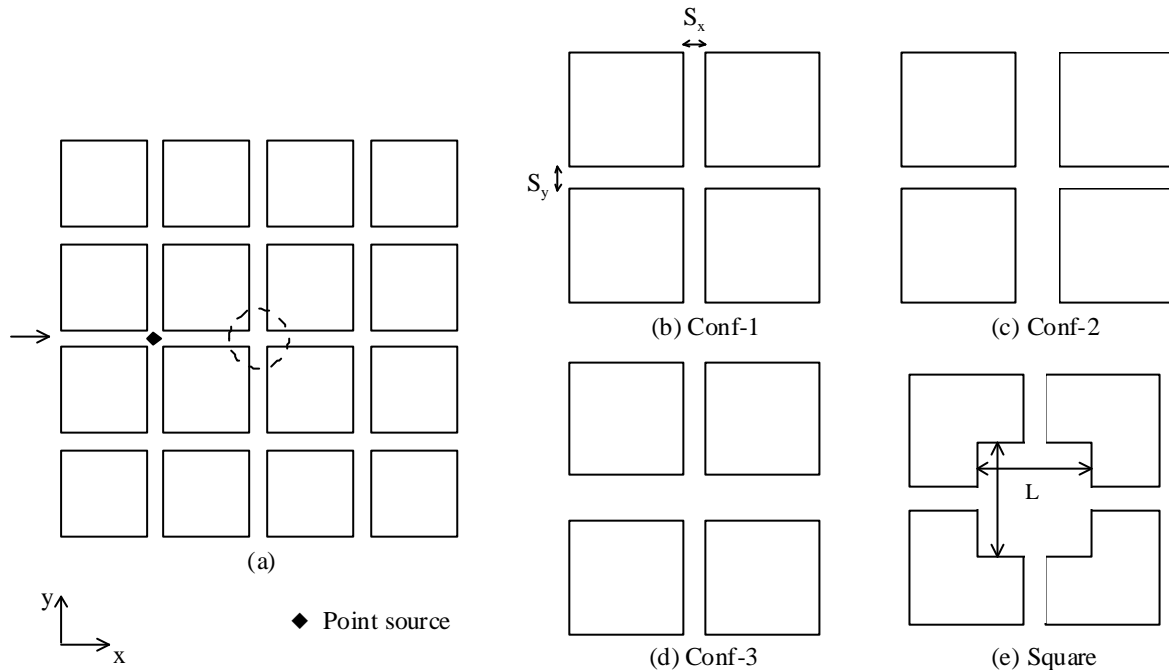


Fig. 1; Wind-tunnel set up and the investigated configurations.

RESULTS

Experimental and numerical investigations have been performed in order to study the flow dynamics within the street intersections for a wind parallel to the axis of the street, i.e. the x -axis; the vectors in the Figure 2 represent the mean velocity field on the horizontal plane $z=H/2$ for the street intersection Conf-1 and Conf-3², as calculated by FLUENT. The flow within the intersection is parallel to the external wind and “drives” the recirculating motion within the adjacent streets; the topology of the flow is similar for the different street configurations, suggesting that for the street spacing $S_x=1$ a typical skimming flow occurs. In Figure 3, the transversal profiles of the mean velocity, non-dimensionalised by the velocity at the boundary layer height U_b , are presented: the numerical results show a good agreement with the experimental data.

Concerning the pollutant dispersion, we investigated experimentally the influence of the intersection layout on the pollutant transport and the exchange phenomena. In Figure 4a, the transversal profiles of the mean concentration, at height $z=H/2$, are plotted for the different

¹ Except for the square configuration, as the domain could not be assumed periodic.

² The configuration Conf-2 is omitted for shortness, as it confirms the behaviour observed in the others.

street intersections and are fitted to a Gaussian profile, as suggested by numerous authors (Macdonald, R. W. et al., 1998; Gailis R. M. et al., 2006):

$$K = K_{\max} \exp\left[-\frac{y^2}{2s_y^2}\right] \quad (2)$$

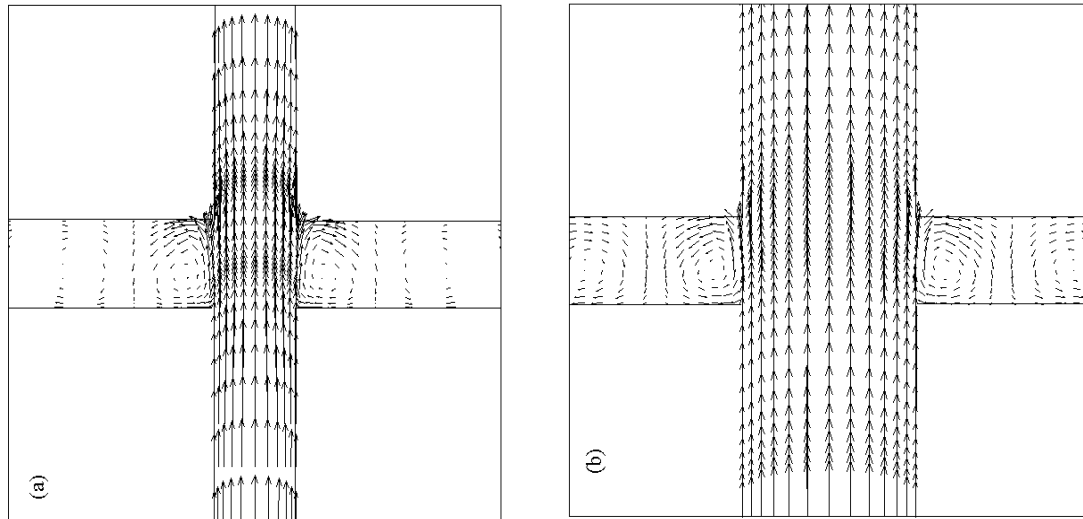


Fig. 2; Mean velocity field in the street intersections at $z=H/2$: (a) Conf-1 and (b) Conf-3.

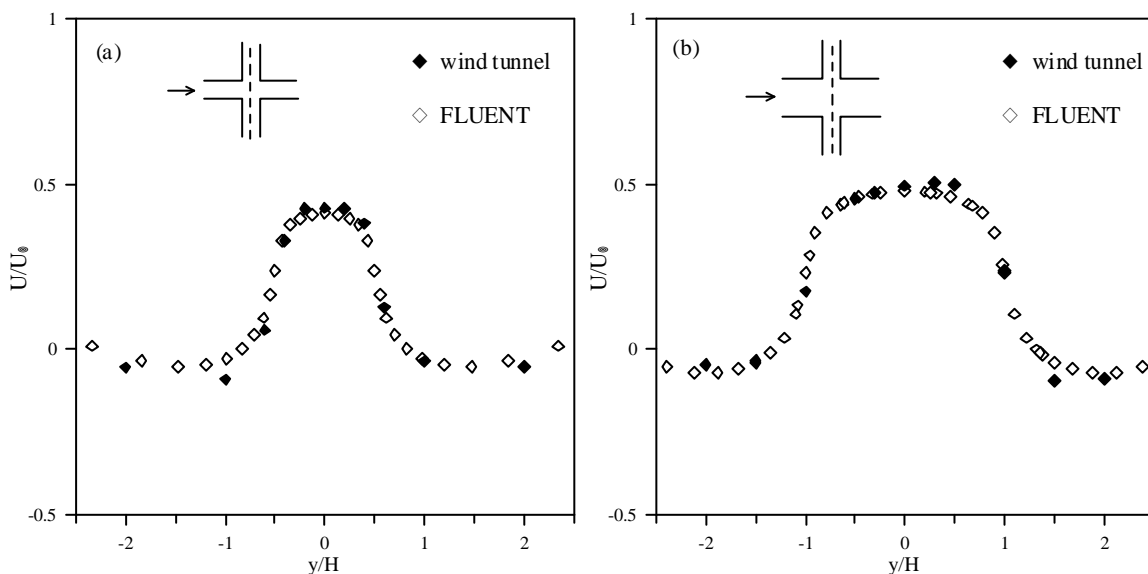


Fig. 3; Mean velocity transversal profiles at $z=H/2$: (a) Conf-1 and (b) Conf-3.

The Gaussian fit describes quite well the concentration distribution within the intersection, while within the adjacent streets a different behaviour is observed, suggesting that the plume spreading is strongly affected by the geometrical layout. The standard deviation σ_y evaluates the horizontal dispersion and seems to be controlled by the street spacing S_x , the geometrical parameter that characterises the dimension of the exchange interface between the intersection and the lateral streets (Figure 4b). For $S_x/H=1$, a skimming flow regime takes place and the flow dynamics along the x -axis and within the adjacent streets are somehow decoupled: a

phenomenon of channelling occurs that limits the pollutant exchange and so the plume spreading; for $S_x/H=2$, a wake-interference flow is supposed that homogenises the pollutants and smoothes the concentration distributions.

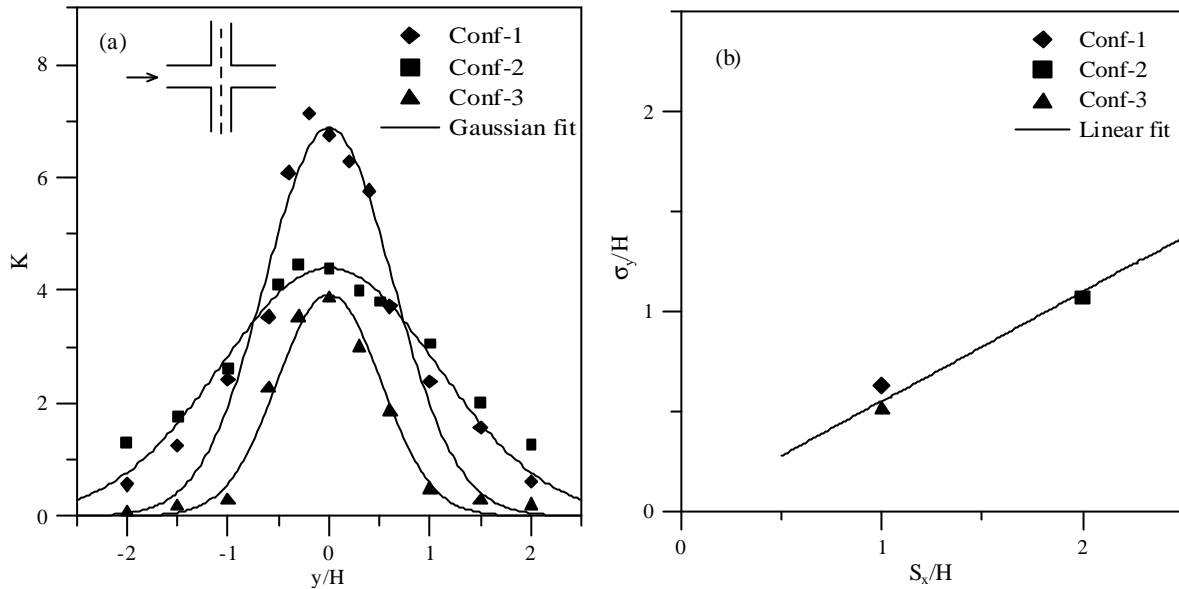


Fig. 4; (a) Transversal mean concentration profiles and (b) σ_y values for the different street intersections

Finally, experimental and numerical investigations have been performed within a square. The mean velocity field calculated by FLUENT on a horizontal plane, at $z=H/2$, is shown in Figure 5 and exhibits two recirculation vortex in the leeward corners. Although the general flow pattern is properly simulated, numerical results don't agree very well with the experimental data, as long as they overestimate the dimensions of the vortex: the numerical profiles suggest that the recirculation cells extend beyond the centre of the intersection, whereas the experimental profiles show they are confined in smaller regions.

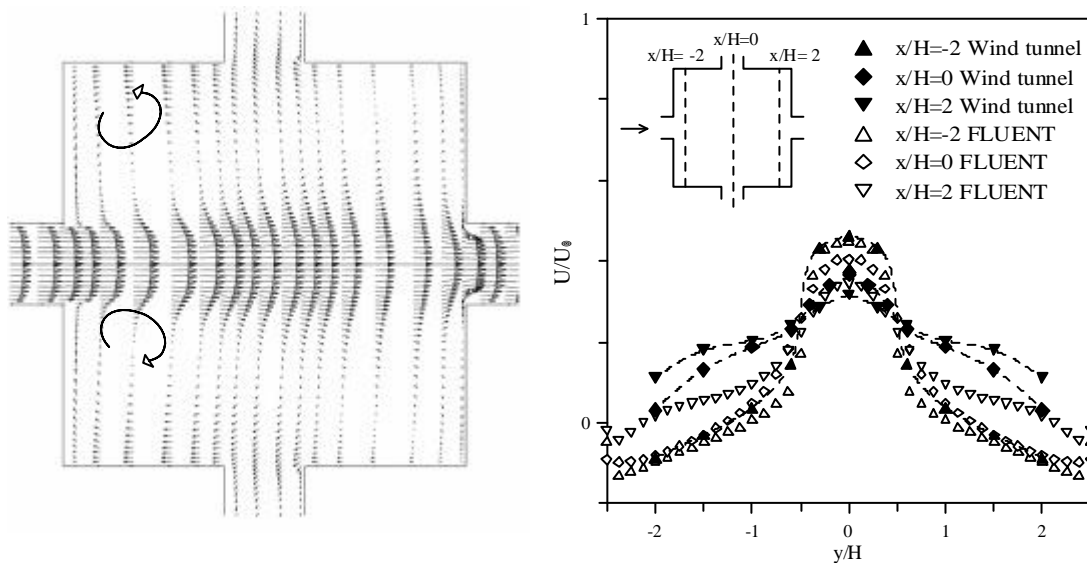


Fig. 5; Mean velocity field at $z=H/2$ (FLUENT) and mean velocity transversal profiles

The presence of a recirculation vortex in the leeward corner is confirmed by the mean concentration field measured in the wind tunnel at $z=H/2$ and displayed in Figure 6: the vortex captures the pollutants and causes higher concentration values in the corners. The transversal profiles of the mean concentration within the square point out two mechanisms of dispersion: the mean motion along the stream-wise axes transports the pollutants outside the square, while the fluctuating component diffuses the pollutants within it and makes homogeneous the concentration.

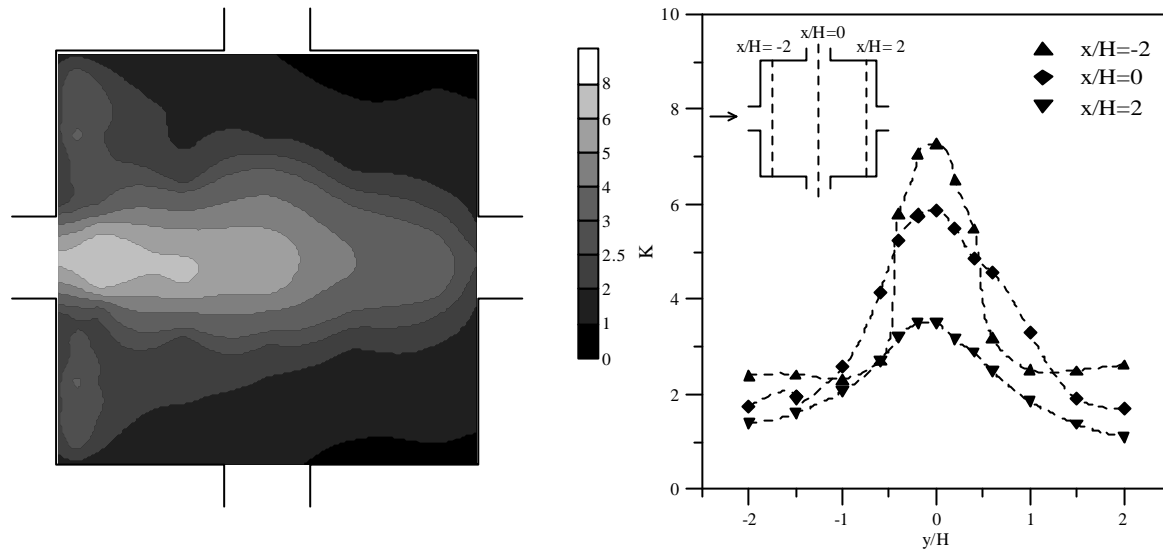


Fig. 7; Mean concentration field at $z=H/2$ (wind tunnel) and mean concentration transversal profiles

CONCLUSIONS

It is evident that the flow pattern and the plume spreading are strongly affected by the geometrical layout. In the case of the street intersections, a skimming flow regime occurs for $S_x/H=1$ and a decoupling between the external flow and the flow within the intersection takes place; the numerical simulations agree very well with the experimental data. The dispersion processes seem to be related to the local generated turbulence. In the case of the square, the larger extent of the interface with the external flow induces more complicated mass and momentum exchange mechanisms. The numerical simulations don't show a good agreement with the experimental results; maybe, a more accurate representation of the boundary layer flow dynamics is required.

REFERENCES

- Dabbert W., W. Hoydysh, M. Schoring, F. Yang, O. Holynskyi, 1995: Dispersion modelling at urban intersection. *Sci. Total Env.* **169**, 93-102.
- Gailis R.M. and Hill A., 2006: A wind-tunnel simulation of plume dispersion within a large array of obstacles. *Boundary-Layer Meteorology* **119**, 289-338.
- Macdonald R.W., Griffiths R.F. and Hall D.J., 1998: A comparison of results from scaled field and wind tunnel modelling of dispersion in arrays of obstacles. *Atmospheric Environment* **32**, 3845-3862.
- Robins A., E. Savory, A. Scaperdas, D. Grigoriadis, 2002: Spatial variability and source-receptor relations at a street intersection. *Water Air Soil Pollut.: Focus.* **2**, 381-393.
- Wang X. and K. F. McNamara, 2007: Effects of street orientation on dispersion at or near urban street intersections. *J. Wind Eng. Ind. Aerodyn.*